Int J Adv Manuf Technol (2009) 43:40–51
DOI 10.1007/s00170-008-1698-8

ORIGINAL ARTICLE

In-process surface roughness prediction system using cutting vibrations in turning

D. R. Salgado · F. J. Alonso · I. Cambero · A. Marcelo

Received: 3 July 2007 / Accepted: 4 August 2008 / Published online: 6 September 2008

Abstract Machining is a complex process in which many variables can affect the desired results. Among them, surface roughness is a widely used index of a machined product quality and, in most cases, is a technical requirement for mechanical products since, together with dimensional precision, it affects the functional behavior of the parts during their useful life, especially when they have to be in contact with other materials. In-process surface roughness prediction is, thus, extremely important. In this work, an in-process surface roughness estimation procedure, based on least-squares support vector machines, is proposed for turning processes. The cutting conditions (feed rate, cutting speed, and depth of cut), parameters of tool geometry (nose radius and nose angle), and features extracted from the vibration signals constitute the input information to the system. Experimental results show that the proposed system can predict surface roughness with high accuracy in a fast and reliable way.

Keywords Surface roughness · Surface quality · Vibration signal · Turning · LS-SVM

D. R. Salgado (✉)
Department of Mechanical, Energetic and Materials Engineering, University of Extremadura,
Sta. Teresa de Jornet 38, 06800 Mérida, Spain
e-mail: drs@unex.es

F. J. Alonso · I. Cambero · A. Marcelo
Department of Mechanical, Energetic and Materials Engineering, University of Extremadura,
Avda. Elvas s/n, 06071 Badajoz, Spain

Nomenclature

v_c	Cutting speed
f	Feed rate
d	Depth of cut
r	Nose radius
A	Nose angle
V_B	Tool flank wear
R_a	Surface roughness
$\mathbf{x}_i$	Input vector
y_i	Scalar output
$\mathbf{w}$	Weight vector
$\varphi(\cdot)$	Nonlinear transformation
b	Bias term
α_i	Lagrange multiplier
$K(\mathbf{x}, \mathbf{x}_i)$	Kernel function
$\mathbf{e}_i$	Random error
C	Regularization parameter
Ω	Kernel matrix
σ	Kernel function parameter
λ_j	jth-eigenvalue of the SSA decomposition

1 Introduction

Surface roughness is a widely used index of a machined product quality and, in most cases, is a technical requirement for mechanical products since achieving the desired surface quality is of great importance for their functional behavior. However, the mechanism of surface roughness formation depends on various uncontrollable factors that make its estimation difficult. Much research time and effort has been devoted to studying surface roughness prediction, from the 1980s [1, 2] until today [3–16]. The full potential of these techniques in

practical applications has yet to be investigated, so that most strategies are based on conservative estimates [17].

Cutting forces and machining vibrations have been reported to be much more significant than other monitoring signals [3–14] in predicting surface roughness. In practice, however, a dynamometer is more expensive and difficult to mount on a lathe than an accelerometer. Machining vibrations play an important role in producing surface roughness [13, 18], but the many parameters that affect them – machine structure, tool type, workpiece material, etc. – complicate their composition.

Recent research on surface roughness prediction [3–14] has had remarkably positive results in predicting surface roughness using vibration in a single direction. Yet, to be resolved, however, is the question of deciding which are the features of the vibration data that are most strongly correlated with surface quality [17, 19]. Another topic of controversy in the literature is the frequency range that needs to be analyzed. While some works have focused on a low-frequency range, others have found it reasonable to make measurements in a higher-frequency range [4, 8, 20].

Given this context, the aims of the present work were to develop an in-process procedure for surface roughness estimation for turning, and to determine which would be significant vibration features to use in an accelerometer-based surface roughness prediction model. We use singular spectrum analysis (SSA) to decompose the cutting vibration signals in order to extract the information most strongly correlated with surface roughness. The least squares version of support vector machines (LS-SVM), a modified version of the standard support vector machines, was used for surface roughness estimation. The experimental results showed SSA to be well suited for processing the vibration signals in order to correlate the information that they contain with surface roughness and confirm that LS-SVM can be used for a fast and reliable surface roughness estimation.

The paper is organized as follows: Section 2 describes the vibration analysis and presents a brief overview of SSA. Section 3 presents the surface roughness prediction strategy and briefly reviews LS-SVM methodology. Section 4 describes the experimental setup, and Section 5 the results. Finally, the conclusions are presented in Section 6.

2 Vibration signal analysis

Turned surface profiles can be divided into a periodic component and a random component. The periodic component is a function that mainly depends on tool shape and feed rate, and the random component is caused by machine vibrations [21]. The difference between real and theoretical surface roughness can be attributed to the influence of such physical and dynamic phenomena as built-up edge, friction of cut surface against tool point, and vibrations [11].

Vibrations have been reported to be fairly strongly correlated with surface roughness [3–12, 17], and various features of vibration signals have been chosen to estimate surface quality. Lin et al. [3] studied the relative motion between the cutting tool and the workpiece on the surface finish profile, using the ratio between the vibration frequency and the spindle rotational speed. Other parameters used have been the RMS of the vibrations (Bonifacio et al. [4]); the directly measured voltage output of the accelerometer (Kirby et al. [6]); the power spectral density of the signal (Abouelatta et al. [8]); and the tool deflection, tool speed, and tool acceleration (Thomas et al. [11, 13]). Jang et al. [5] and Cheung et al. [12] studied the relative cutting vibrations between tool and workpiece and showed that surface roughness along the workpiece has specific frequency components in the lower-frequency range that are closely related to the natural frequencies of the spindle-workpiece system in the high-frequency range. Kirby et al. [16] collected the vibration signals in positive and negative directions along their respective axes, and then, these data were transformed into absolute values, or amplitudes of vibration. This method enabled the researchers to determine a mean amplitude of vibration using accelerations in both directions along the axes. Other works [7, 9, 14, 19] have directly used the amplitude of the vibrations.

The present work uses a novel nonparametric technique – SSA – to extract information from the vibration signal. This technique was used by the current authors in the area of tool condition monitoring [22] to extract information from vibration signals with successful results. The following section will briefly describe this advanced signal processing technique.

2.1 Background: SSA

SSA is a nonparametric technique of time series analysis based on principles of multivariate statistics. It decomposes a given time series into a set of independent additive time series. Fundamentally, the method projects the original time series onto a vector basis obtained from the series itself, following the procedure of principal component analysis. The set of series resulting from the decomposition can be interpreted as a slowly

varying trend representing the signal mean at each instant, a set of periodic series, and an aperiodic noise [23]. Wang et al. [24] were the first to apply SSA to the diagnosis of rotating machinery failures using vibration signals, and Salgado et al. used SSA to extract the information of vibration signals [22] and sound signals [25, 26] most strongly correlated with tool flank wear.

The SSA method builds a matrix, called the trajectory matrix (**X**), from the original time series in a process called *embedding*. This matrix consists of vectors obtained by means of a sliding window that traverses the series. The trajectory matrix is then subjected to a singular value decomposition (SVD). The SVD decomposes the trajectory matrix into a sum of unit-rank matrices known as elementary matrices ($\mathbf{E}_i$). At this step, the method calculates the eigenvalues of a matrix (**S**) constructed with the above trajectory matrix ($\mathbf{S}=\mathbf{X}\cdot\mathbf{X}^T$). The plot of the eigenvalues in decreasing order is called the singular spectrum, and it gives the method its name. The correspondence between singular spectrum (obtained with SSA) and frequency spectrum is the basis of this processing technique. It is important to bear in mind that the SSA decomposition is not based on the frequency but on the SVD of the trajectory matrix of the time series, which is what gives the method its power in signal processing. A more detailed explanation may be found in Golyandina et al. [23].

In the present work, SSA is applied to the decomposition of the radial (X direction), tangential (Y direction), and feed (Z direction) vibration signals in order to extract the most valuable information that they contain with respect to surface roughness. Various studies [3–12] have found strong correlation between the cutting vibrations and surface roughness in turning.

The vibration signals acquired during the turning process were decomposed using SSA, implementing the algorithm of Golyandina et al. [23] in the Matlab environment. Application of the SSA algorithm only requires the choice of the window length (that of the sliding window), and the same window length ($L = 5$) used in [22] was found to be appropriate for the present task also.

The properties of SSA decomposition allow one to obtain a strategy to estimate surface roughness, since changes in the frequency spectra of the vibration signals produce changes in their singular spectra, with the advantage that the singular spectrum provides five values (the eigenvalues of the singular spectrum) with which to evaluate the frequency spectrum. In other words, the singular spectrum allows one to detect changes in the signal, since it represents in a compact manner the frequency spectrum of the signal. Another question that is important to bear in mind is that the low frequencies of the signal are represented in the singular spectrum by the largest eigenvalues and the high frequencies by the smallest eigenvalues.

Figure 1a shows the first 1,000 data points of one of the recorded feed vibration signals, and Fig. 1b shows its singular spectrum. The singular spectrum shows the five eigenvalues ($L = 5$) into which the signal is decomposed. The first eigenvalue represents the low frequency and the fifth the high frequency of the signal [23]. Figure 1c shows two different singular spectra obtained under the same cutting conditions, and resulting in different surface roughnesses, as is shown in the figure. Figure 1d represents the percentage change of the eigenvalues shown in Fig. 1c. In particular, for this case, the percentage variations of the first and second eigenvalues, which are the greatest variations as shown in Fig. 1d, are 17.8% and 10.7%, respectively. The other percentages are 6.9%, 2.7%, and 1.9% for the third to fifth eigenvalues, respectively.

Similarly, Fig. 1e shows two different singular spectra obtained under the same cutting conditions but with different tool flank wear, and resulting in different surface roughnesses, too. In these cases, in which the flank wear is different, the greatest variations in the singular spectra are in the eigenvalues corresponding to higher frequencies, mainly in the third eigenvalue, as is shown in Fig. 1f. In particular, the percentage variation of the third eigenvalue is 14.5%.

In both cases (Fig. 1c and e), the changes in the eigenvalues are greater in the eigenvalues corresponding to the frequency range in which the amplitudes undergo greater changes. These changes in the eigenvalues are probably due to factors such as friction, workpiece length, chip-thickness variation, etc., and to tool wear [22]. In any case, these changes in the eigenvalues of the singular spectra correspond to different resulting surface roughnesses and, hence, make it possible to obtain a strategy for surface roughness estimation.

Comparing the singular spectra obtained for each of the vibration signals (radial, tangential, and feed directions), one notes that the greatest changes in the eigenvalues when machining under the same cutting conditions but different tool wear are observed in the SSA decomposition of the feed vibration. This seems to be coherent with the findings of Kirby et al. [19] and Dimla [27] that the feed vibrations are somewhat more strongly correlated with tool flank wear than the others.

3 Surface roughness estimation: LS-SVM

The estimation technique used in this work is the LS-SVM—a reformulated version [28, 29] of standard

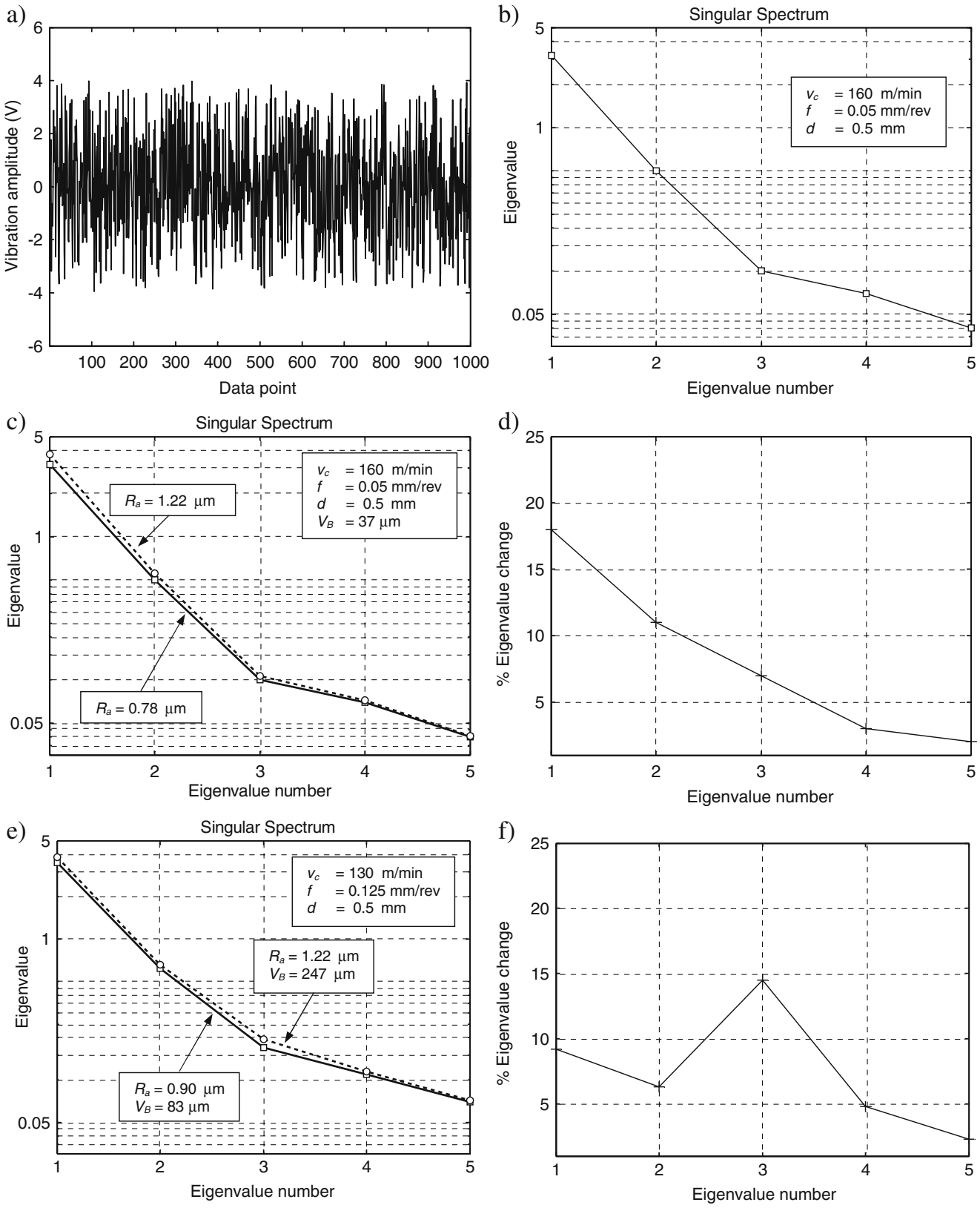

Fig. 1 **a** The first 1,000 data points of one of the recorded feed vibration signals, **b** the corresponding singular spectrum for a window length of $L = 5$ (eigenvalues on logarithmic scale), **c** two singular spectra under the same cutting conditions but different R_a, **d** percentage change of eigenvalues of the two singular spectra of **c**, **e** two singular spectra under the same cutting conditions but different V_B and R_a, **f** percentage change of eigenvalues of **e**

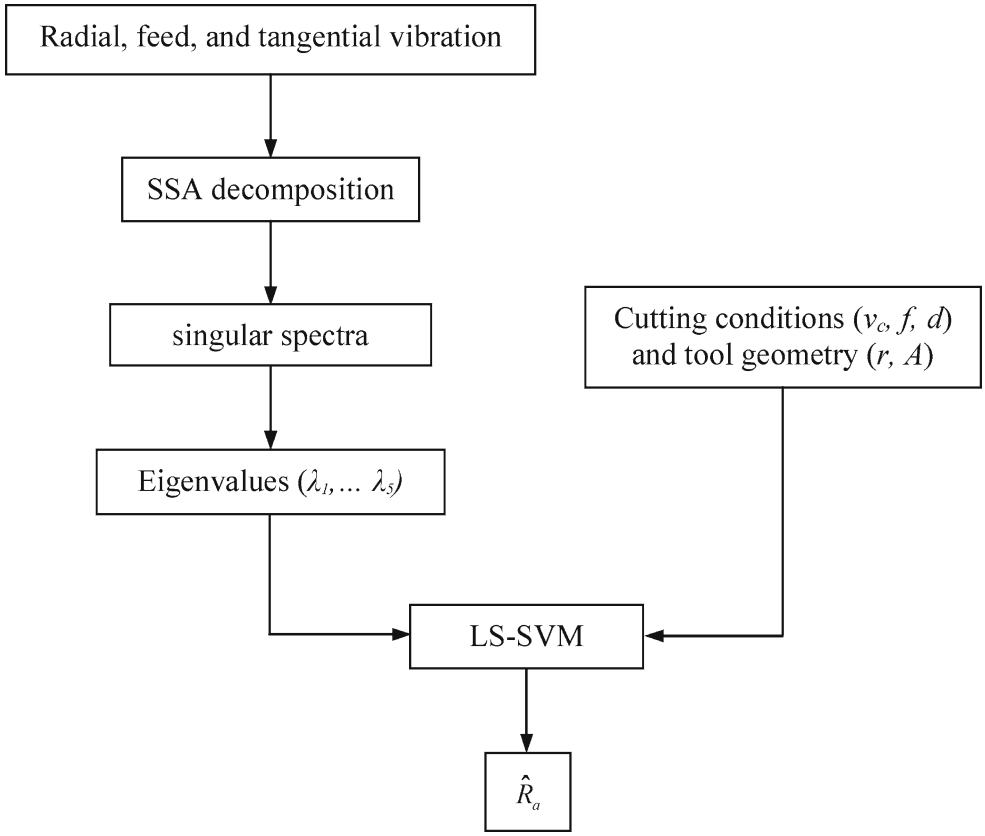

Fig. 2 Scheme of the surface roughness estimation process

support vector machines (SVM). The technique is closely related to regularization networks, Gaussian processes [30], and Fisher discriminant analysis with kernels [31]. Its main advantage is that it is computationally more efficient than the standard SVM method. Figure 2 is a schematic diagram of the surface roughness estimation process proposed in the present work.

3.1 Background: LS-SVM

SVM is a novel machine-learning tool and a powerful methodological approach to solving problems in nonlinear classification [32]. It is especially useful for classification and prediction with small sample sizes [31]. Motivated by statistical learning theory, the approach has led to a class of algorithms characterized by the use of nonlinear kernels, a high capacity for generalization, and the sparseness of the solution. The main advantage of LS-SVM (that it is computationally more efficient than the standard SVM method) is that LS-SVM training only requires the solution of a set of linear equations instead of the long and computationally difficult quadratic programming problem involved in standard SVM. SVM and LS-SVM have recently been successfully used in the tool condition field [26, 33–35]. In the following, we shall give the essentials of the formulation of LS-SVM.

Consider a training set $\{\mathbf{x}_i, y_i\}_{i=1}^{N}$, where $\mathbf{x}_i \in \Re^p$ represents a p-dimensional input vector and $y_i \in \Re$ is a scalar measured output that represents the y_i system output. The goal is to construct a function $y = f(\mathbf{x})$ that represents the dependence of the output y_i on the input $\mathbf{x}_i$. The LS-SVM model is of the following form:

$$y = \mathbf{w}^T \varphi(\mathbf{x}) + b\,, \tag{1}$$

where $\mathbf{w}$ is the weight vector and b is the bias term. In the present work, this function is constructed with the input $\mathbf{x}_i$ being the information presented to estimate the surface roughness (see Section 3.2) and y_i is the corresponding surface roughness.

This regression model can be constructed using a nonlinear mapping function $\varphi(\cdot)$. By mapping the original input data onto a high-dimensional space, the nonlinear separable problem becomes linearly separable in space. The function $\varphi(\cdot) : \Re^p \to \Re^h$ is a mostly nonlinear function that maps the data into a higher – possibly infinite – dimensional feature space. The main difference from the standard SVM is that LS-SVM involves equality constraints instead of inequality constraints and works with a least squares cost function [32]. The

optimization problem and the equality constraints are defined by the following equations:

$$\min J(\mathbf{w}, \mathbf{e}) = \frac{1}{2}\mathbf{w}^T\mathbf{w} + C\frac{1}{2}\sum_{i=1}^{N} e_i^2 \tag{2}$$

subject to:

$$y_i = \mathbf{w}^T\varphi(\mathbf{x}_i) + b + e_i, \qquad i = 1, ..., N$$

where e_i is the random error and $C \in \Re^+$ is a regularization parameter in optimizing the trade-off between minimizing the training errors and minimizing the model's complexity. The objective is now to find the optimal parameters that minimize the prediction error of the regression model (1). The optimal model will be chosen by minimizing the cost function (2) where the errors e_i are minimized [32]. This formulation corresponds to the regression in the feature space and, since the dimension of the feature space is high, possibly infinite, this problem is difficult to solve. Therefore, to solve this optimization problem, the following Lagrange function is constructed:

$$L(\mathbf{w}, b, \mathbf{e}; \boldsymbol{\alpha}) = J(\mathbf{w}, \mathbf{e}) - \sum_{i=1}^{N} \alpha_i \left\{\mathbf{w}^T\varphi(\mathbf{x}_i) + b + e_i - y_i\right\} \tag{3}$$

where $\boldsymbol{\alpha} = [\alpha_1, \alpha_2, ..., \alpha_n]$ are the Lagrange multipliers. The solution of Eq. 3 can be obtained by partially differentiating with respect to $\mathbf{w}$, b, e_i, and α_i, i.e.,

$$\frac{\partial L}{\partial \mathbf{w}} = 0 \rightarrow \mathbf{w} = \sum_{i=1}^{N} \alpha_i\varphi(x_i), \tag{4}$$

$$\frac{\partial L}{\partial b} = 0 \rightarrow \sum_{i=1}^{N} \alpha_i = 0, \tag{5}$$

$$\frac{\partial L}{\partial e_i} = 0 \rightarrow \alpha_i = Ce_i, \qquad i = 1, ..., N, \tag{6}$$

$$\frac{\partial L}{\partial \alpha_i} = 0 \rightarrow \mathbf{w}^T\varphi(x_i) + b + e_i - y_i = 0, \qquad i = 1, ..., N. \tag{7}$$

In matrix form, the above equations can be expressed as

$$\begin{bmatrix} 0 & \vec{\mathbf{1}}^T \\ \vec{\mathbf{1}} & \boldsymbol{\Omega} + C^{-1}\boldsymbol{I} \end{bmatrix} \begin{bmatrix} b \\ \boldsymbol{\alpha} \end{bmatrix} = \begin{bmatrix} 0 \\ \mathbf{y} \end{bmatrix} \tag{8}$$

where

$$\mathbf{y}^T = \left[y_1, y_2, ..., y_N\right],$$

$$\vec{\mathbf{1}}^T = [1, ..., 1],$$

$$\boldsymbol{\alpha}^T = [\alpha_1, \alpha_2, ..., \alpha_N],$$

$$\Omega_{ij} = K(\mathbf{x}_i, \mathbf{x}_j) = \varphi^T(\mathbf{x}_i)\varphi(\mathbf{x}_j), \qquad j = 1, ..., N.$$

and where $(K(\mathbf{x}_i, \mathbf{x}_j))$ is the kernel function, and $\boldsymbol{\Omega}$ is the kernel matrix. Finally, the estimated values of b and α_i, i.e., $\hat{b}$ and $\hat{\alpha}_i$, can be obtained by solving the linear system Eq. 8, and the resulting LS-SVM model can be expressed as

$$y = f(\mathbf{x}) = \sum_{i=1}^{N} \hat{\alpha}_i K(\mathbf{x}, \mathbf{x}_i) + \hat{b} \tag{9}$$

where K($\mathbf{x}$,$\mathbf{x}_i$) is a kernel function. In the present work, we chose the nonlinear radial basis function (RBF) kernel:

$$K(\mathbf{x}, \mathbf{x}_i) = exp\left(-\frac{1}{2\sigma^2}\left\|\mathbf{x} - \mathbf{x}_i\right\|^2\right) \tag{10}$$

where σ is the scale factor for tuning. In comparison with some other feasible kernel functions, the RBF is a more compact supported kernel and able to shorten the computational training process and improve the generalization performance of LS-SVM, a feature of great importance in designing a surface roughness prediction system for practical application.

3.2 Surface roughness estimation method

The eigenvalues of the SSA decomposition of the cutting vibrations together with the cutting conditions and the information relative to tool geometry constitute the vector $\mathbf{x}_i$, which is used to describe the relationship between this information and R_a (the output of the model y_i) using LS-SVM (see Fig. 2). These constitute the input–output pairs to train LS-SVM. The experimental data used to construct the model are given in Table 1.

It is not known beforehand which values of the regularization parameter C and σ from the kernel function are the best for the problem. Consequently, to achieve a high level of performance with LS-SVM models, C and σ have to be tuned. In the present work, we used a grid-search technique to tune these two parameters, applying fivefold cross-validation to the training set (see Table 1) to find the optimal parameter values. The procedure was implemented in the LS-SVMlab1.5

Table 1 Training data set

	v_c (m/min)	f (mm/rev)	d (mm)	r (mm)	A	V_B (μm)	Replicates R_a (μm)			Mean R_a (μm)
1	90	0.05	0.5	0.8	80	87	1.96	1.69	1.77	1.81
2	90	0.05	1	0.8	35	121	2.01	1.76	1.87	1.88
3	90	0.125	0.5	0.8	35	53	1.59	1.79	1.87	1.75
4	90	0.05	1	0.8	80	25	1.81	1.64	1.77	1.74
5	90	0.125	1	0.4	60	109	1.39	1.62	1.61	1.54
6	90	0.05	0.5	0.4	35	215	2.14	1.95	2.11	2.06
7	90	0.125	0.5	0.4	60	123	1.43	1.68	1.57	1.56
8	110	0.125	0.5	0.4	60	174	1.55	1.52	1.37	1.48
9	110	0.20	1	0.8	80	127	3.58	3.24	3.29	3.37
10	110	0.125	0.5	0.4	35	96	1.76	1.65	1.78	1.71
11	110	0.20	0.5	0.8	35	59	4.57	4.75	5.12	4.81
12	110	0.125	1	0.4	60	28	1.79	1.73	1.91	1.81
13	110	0.05	1	0.8	35	56	1.21	1.49	1.10	1.27
14	110	0.125	0.5	0.4	35	114	1.52	1.68	1.54	1.58
15	130	0.125	0.5	0.8	80	165	1.57	1.50	1.36	1.48
16	130	0.125	1	0.4	35	37	1.71	1.69	1.83	1.74
17	130	0.05	1	0.8	80	131	1.67	1.44	1.74	1.62
18	130	0.05	0.5	0.4	60	156	0.93	1.02	0.97	0.97
19	130	0.125	1	0.8	35	85	1.70	1.78	1.42	1.63
20	130	0.05	0.5	0.4	60	144	0.72	1.05	0.90	0.89
21	130	0.125	0.5	0.4	35	78	1.63	1.75	1.70	1.69
22	160	0.125	0.5	0.4	60	28	1.15	0.90	0.98	1.01
23	160	0.20	1	0.8	35	185	3.12	3.46	3.98	3.19
24	160	0.125	0.5	0.4	60	26	1.07	1.18	1.02	1.09
25	160	0.05	1	0.8	80	59	1.22	1.35	1.61	1.39
26	160	0.125	1	0.4	60	82	1.21	1.14	1.32	1.22
27	160	0.05	0.5	0.8	35	119	0.72	1.00	0.92	0.88
28	160	0.125	0.5	0.4	35	153	1.12	1.19	1.21	1.17
29	180	0.20	0.5	0.4	60	88	1.12	0.95	1.15	1.07
30	180	0.125	1	0.8	80	34	1.01	0.97	1.07	1.02
31	180	0.125	1	0.4	35	74	1.38	1.57	1.41	1.45
32	180	0.20	0.5	0.8	80	93	3.25	3.01	3.10	3.12
33	180	0.125	0.5	0.4	60	162	1.12	1.35	1.45	1.29
34	180	0.125	1	0.8	35	27	1.70	1.62	1.40	1.57
35	180	0.125	0.5	0.4	35	55	1.34	1.43	1.39	1.39

Toolbox. A good result was obtained with $C = 15.893$ and $\sigma = 0.257$, and its performance will be described in Section 5. Once it has learned the correlation between input information (processed information from vibrations, cutting conditions, and tool geometry) and output information (R_a), the trained LS-SVM is used to estimate the surface roughness following the process outlined in Fig. 2. A more detailed description of LS-SVM can be found in [32].

4 Experimental setup

Figure 3 is a schematic diagram of the experimental setup. The accelerometers (Kistler type 8742A50 and Kistler 5807 A amplifiers) were placed close to the tool to measure the cutting vibrations. The signals from the accelerometers were processed and logged by means of a data acquisition card (DSPT Siglab model 20–42) connected directly to a PC (Pentium IV 2.4 MHz) driven from the Matlab environment. The signals were sampled at a rate of 10 kHz for 150 ms.

AISI 8620 steel was used as the workpiece material in the experiments, and various tools (TiN-coated carbide inserts) of ISO types CCMT 120404, CCMT 120408, TCMT 110204, VCMT 160404, and VCMT 160408 were used. Table 1 lists the experimental data used to train the proposed LS-SVM model, and Table 2 shows the validation data. For each experiment, the surface roughness was measured at three equally spaced locations around the circumference of the workpieces. The mean value, given in Table 1, was used as the output value (y_i) in the estimation model. The surface roughness was measured with a Hommel-tester T1000 rugosimeter. The cut-off length was fixed at 0.8 mm and the total length measured was 2.4 mm.

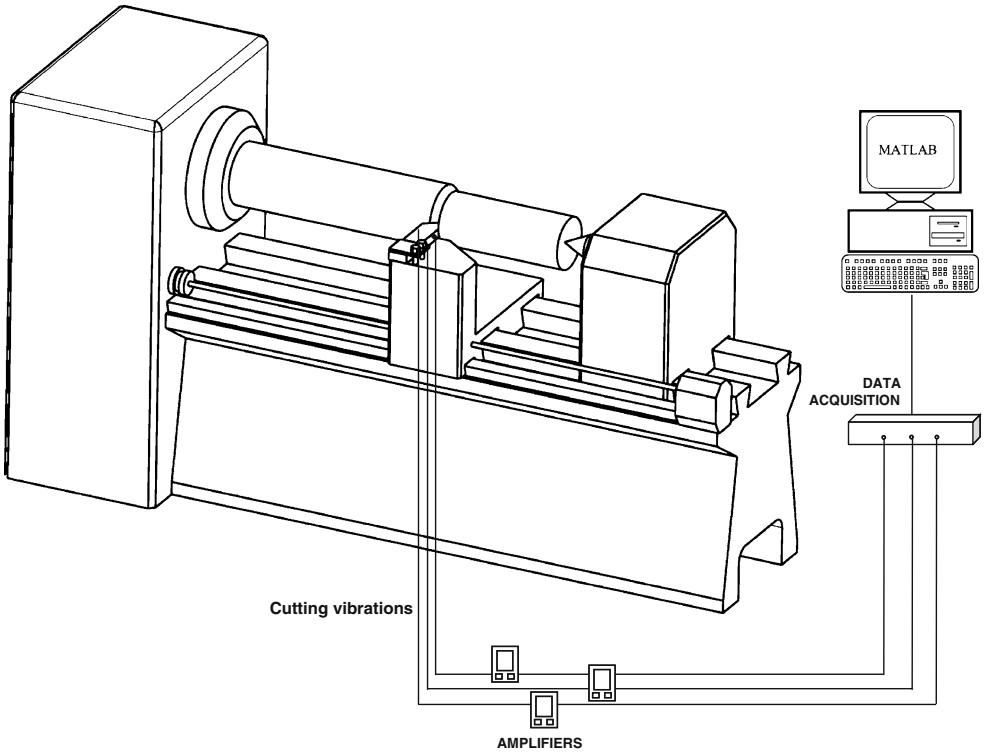

Fig. 3 Diagram of the experimental set-up

5 Results and discussion

The experimental design described in the previous section was used to construct the surface roughness prediction model for turning operations using LS-SVM. After the LS-SVM model was trained on the information in the vectors $\mathbf{x}_i$ of the training data (see Table 1), the method was validated using the experimental conditions given in Table 2. Again, for each experiment, the surface roughness was measured at three equally spaced locations around the circumference of the workpieces. In both the training and validation steps, the

Table 2 Validation data set

	v_c (m/min)	f (mm/rev)	d (mm)	r (mm)	A	V_B (μm)	Replicates R_a (μm)			Mean R_a (μm)
1	90	0.05	1	0.8	35	76	1.95	2.07	1.91	1.98
2	90	0.125	1	0.4	80	68	1.53	1.38	1.57	1.49
3	90	0.125	0.5	0.4	60	51	1.72	1.55	1.62	1.63
4	90	0.05	0.5	0.8	80	108	1.64	1.78	1.67	1.70
5	110	0.125	0.5	0.4	60	89	1.57	1.65	1.54	1.59
6	110	0.20	0.5	0.8	35	153	4.77	4.53	4.47	4.59
7	110	0.125	1	0.4	60	123	1.52	1.63	1.55	1.57
8	110	0.05	1	0.8	35	181	1.31	1.22	1.49	1.34
9	130	0.125	0.5	0.8	80	93	1.61	1.47	1.70	1.59
10	130	0.05	1	0.8	80	25	1.72	1.79	1.63	1.71
11	130	0.125	0.5	0.4	35	37	1.53	1.49	1.68	1.57
12	130	0.05	1	0.4	60	56	1.97	1.84	1.81	1.87
13	160	0.125	0.5	0.4	60	124	1.09	1.21	1.16	1.15
14	160	0.05	1	0.8	80	96	1.58	1.29	1.37	1.41
15	160	0.05	0.5	0.8	35	43	0.88	1.03	0.97	0.96
16	160	0.125	0.5	0.4	35	65	1.37	1.23	1.34	1.31
17	180	0.125	0.5	0.4	60	76	1.30	1.34	1.18	1.27
18	180	0.20	0.5	0.8	80	159	2.93	3.12	2.87	2.97
19	180	0.125	1	0.8	35	56	1.62	1.76	1.65	1.68
20	180	0.125	0.5	0.4	35	76	1.35	1.47	1.53	1.45

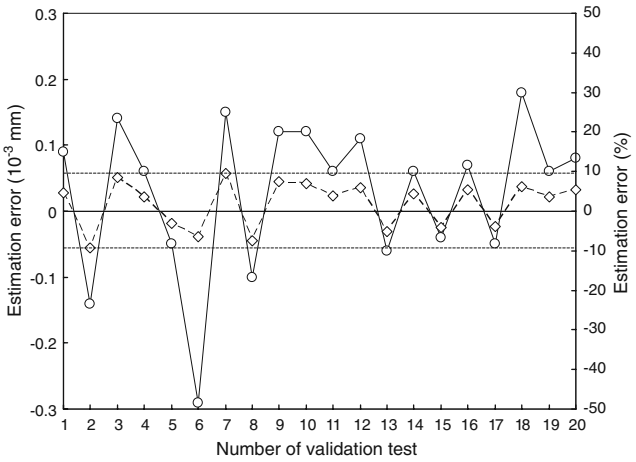

Fig. 4 Estimation errors: *continuous line*, error $\times 10^{-3}$ (mm); *dashed line*, error as percentage

output presented to the model was the mean value of R_a, given in Tables 1 and 2, respectively.

Figure 4 shows the estimation errors, i.e., the differences between the predicted surface roughness ($\hat{R}_a$) and the measured one (R_a) for each of the validation experiments (see Table 2). The mean error of the absolute values of the estimation errors was 5.74%, which indicates good agreement between the input information and the surface roughness prediction. In particular, the results showed that there exists a close relationship between the cutting conditions (feed rate, cutting speed, depth of cut), tool geometry (nose radius and nose angle), SSA decomposition of the vibration signals (eigenvalues of the singular spectra), and surface roughness.

It is important to bear in mind that the proposed surface roughness prediction model takes into account the effects of tool flank wear in cutting vibrations by means of the eigenvalues obtained in the SSA decomposition of the cutting vibrations [22]. This is an important consideration in the development of a surface roughness prediction system since, although flank wear formation alone is not sufficient to explain surface roughness [4], it is also influenced and caused by tool wear [4, 5, 17], and, as noted above, the SSA decomposition carries information about tool condition [22]. Indeed, a notable conclusion in the review of Bernardos et al. [17] is that the integration of tool wear into existing roughness models can improve their accuracy, especially in cases of finishing turning. Nevertheless, it is important to note that the effects of tool wear depend on the combination of workpiece and tool material. For example, Ghani et al. [7] found no significant effect of tool wear on roughness using nodular cast iron and a ceramic tool.

Another interesting finding was that different values of the cutting conditions and tool geometry have different influences on the surface roughness estimate. Table 3 summarizes these results, giving the mean error and the standard deviation of the estimation errors obtained for each of the specific cutting conditions and tool geometries of the validation experiments (see Table 2). For example, the error for the lowest cutting speed (90 m/min) was 6.52%, which is the mean of the estimation errors obtained in the validation experiments 1–4 (Table 2). This error is greater than the mean error obtained for all the validation experiments (5.74%). For the greatest cutting speed (180 m/min), however, the mean error was only 4.77%. Table 3 also gives the standard deviation of the estimation errors, which was 1.97% for all the validation data (Table 2). In interpreting these results, one must take into account that the cutting conditions were not studied by combining them with all the other conditions (see Table 2). Nevertheless, one can deduce from Table 3 that the mean estimation error increases as cutting speed and nose radius decrease. The other parameters (feed rate,

Table 3 Effects of cutting conditions and tool geometry on the surface roughness estimation errors

	Mean error (%)	Standard deviation (%)
Cutting speed		
90	**6.52**	**2.90**
110	**6.62**	**2.67**
130	**6.07**	1.65
160	4.75	0.62
180	4,77	1.20
Validation data	5.74	1.97
Depth of cut		
0.5	5.27	1.67
1	**6.46**	**2.29**
Validation data	5.74	1.97
Nose angle		
35	5.09	1.33
60	**6.05**	**2.54**
80	**5.98**	**2.69**
Validation data	5.74	1.97
Feed rate		
0.05	5.26	1.53
0.125	**5.97**	**2.40**
0.20	**6.19**	0.18
Validation data	5.74	1.97
Nose radius		
0.4	**6.04**	**2.34**
0.8	5.44	1.60
Validation data	5.74	1.97

Table 4 Effects of cutting conditions, tool geometry, and vibrations on the surface roughness estimates

Prediction model	Cutting conditions v_c, f, d	Tool geometry r, A	Radial vibration	Tangential vibration	Feed vibration	Mean error (%)	Standard deviation (%)
1	X	X	X			7.78	3.67
2	X	X		X		7.57	3.35
3	X	X			X	7.24	3.46
4	X	X	X	X		6.78	3.61
5	X	X	X		X	6.69	3.23
6	X	X		X	X	6.54	3.30
7	X	X	X	X	X	5.74	1.97
8	X		X	X	X	7.58	4.35
9	X			X	X	9.73	5.57
10	X		X	X		9.83	5.86
11	X				X	10.68	7.56
12	X		X			10.94	8.01

depth of cut, and nose angle) have the opposite effect on the estimation error, i.e., the error increases as they increase. Mean errors and standard deviations greater than the corresponding values obtained with all the validation experiments (5.74% and 1.97%, respectively) are given in bold face in Table 3.

As several workers have pointed out, surface quality not only depends on cutting conditions but also on tool geometry, tool wear, vibrations, chip deformation, and side flow [3–6, 8, 14, 17]. In order to detect which of these parameters is most strongly correlated with surface roughness, we constructed 12 prediction models using different input information (see Table 4). All the models were trained with the data of Table 1 and then validated with the data of Table 2 (using only the input data marked with a cross in Table 4), following the procedure described in Section 3. Table 4 presents the results obtained with each model. The model proposed in the present work, described in Section 3.2, was model 7 (Table 4), which uses the cutting conditions, tool geometry parameters, and vibration signals in all three directions.

One can deduce interesting considerations for the development of a surface roughness prediction system from the results presented in Table 4. For example, models constructed without taking into account tool geometry (models 8–12) yield poorer results even when using vibrations in all three directions (model 8). In this last case, the estimation error was greater by almost 2%, and the standard deviation was much greater than with model 7.

The rest of the models (excluding models 7 and 8) only use one or two vibrations. One observes that using two vibration signals gives a greater success rate than using only one, but lower than when using all three vibrations. As one observes from Table 4, there was no clear evidence for deciding which vibration signal is the most strongly correlated with surface roughness (compare the results of models 1–3, 11, and 12). Indeed, their estimation errors and standard deviations were quite similar. In view of these results, it can be concluded that, to decide on the input information, i.e., on how many vibration signals to use to develop the surface roughness prediction system, it is necessary to take into account the unavoidable trade-off between accuracy and system cost.

Figure 5 shows a comparison of the cost and performance (mean estimation error) of different systems. The errors are the lowest obtained in the systems of Table 4 for the models that use one, two, or three vibrations whose errors are 7.24%, 6.54%, and 5.74%, respectively. The total cost in Fig. 5 for each of the systems is the result of the cost of the vibration analyzer and of the accelerometers used. The costs of the systems were calculated by taking as reference that the cost of the vibration analyzer (the greatest cost in

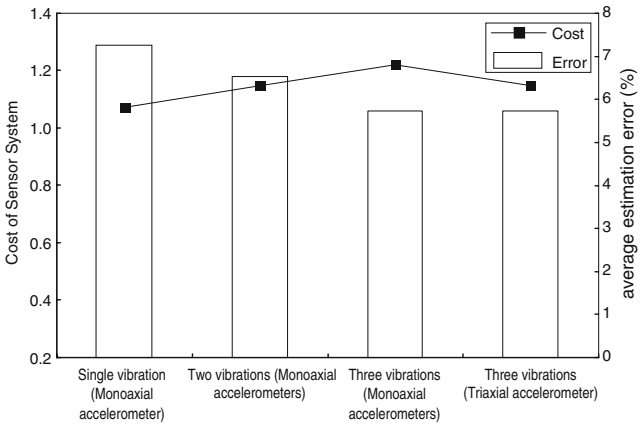

Fig. 5 Cost and performance comparison of surface roughness prediction systems

the sensor system) is equal to unity and by choosing a standard vibration analyzer. The differences between costs are therefore only due to the cost of the accelerometers.

From the information presented in Fig. 5 and the data of Table 4, one can conclude that, although the cost of systems that use only a single vibration signal (monoaxial accelerometer) is less than the others, their estimation errors are greater. Moreover, the cost of systems measuring two vibrations (two monoaxial accelerometers) is almost the same as that of systems equipped with a triaxial accelerometer, but the estimation error of the latter and its standard deviation are less. For this reason, it can be concluded that, in economic and efficiency terms, surface roughness prediction systems based on vibration signals must use triaxial vibration measurement (triaxial accelerometer).

Comparing this procedure with others proposed in literature, three main remarks must be noted. The first one is relative to the use of SSA, since this technique does not require to make any assumption to process the signal, as it is in the case of wavelets, with the necessary selection of a mother wavelet function. The second remark is that the mean estimation error obtained is similar to the errors obtained in other works; however, many of them have a greater cost, something that makes them less appropriate for their industrial application. Finally, it is important to note that the computing time of this estimation procedure is 0.97 s, i.e., the time consumed by the system between the signals acquisition and the output (estimation of R_a). The time computing is taken into account for only a few works in this field of research; however, there are no works publishing their final computing times; they also propose ways to further reduce them, as Luo et al. [36]. In any case, this computing time makes this approach viable for its industrial application.

Finally, it can be concluded that the proposed surface roughness estimation procedure is easy to implement in practice since it only requires the implementation of the accelerometer, and the code of the advanced signal processing technique used in this work has been uploaded by the authors to mathworks.com, and LS-SVM is implemented in Matlab. Therefore, all the necessary tools to implement this approach are available for the research community.

6 Conclusions

We have presented a surface roughness prediction system for turning using the cutting conditions (cutting speed, feed rate, and depth of cut), the tool geometry (nose radius and nose angle), and the vibrations during machining as input information. The principal contributions can be summarized as follows:

- The SSA decomposition of the machining vibrations, i.e., the eigenvalues of the singular spectra of the vibrations, provides invaluable information for use in an accelerometer-based surface roughness prediction system.
- Based on the results of the study, and on the trade-off between cost and estimation error of different systems (see Table 4 and Fig. 5), the use of a triaxial accelerometer is recommended for the development of an accelerometer-based surface roughness prediction system.
- The accuracy of a surface roughness prediction system based on cutting vibrations might be improved by including input information about tool geometry, as well as cutting conditions.
- The results showed that the estimation method used – the LS-SVM – is appropriate for the task of roughness prediction.

References

1. Selvam MS (1975) Tool vibration and its influence on surface roughness in turning. Wear 35(1):149–157
2. Lasota A, Rusek P (1983) Influence of random vibrations on the roughness of turned surfaces. J Mech Work Technol 7(3):277–284
3. Lin SC, Chang MF (1998) A study on the effects of vibrations on the surface finish using a surface topography simulation model for turning. Int J Mach Tools Manuf 38:763–782
4. Bonifacio MER, Diniz AE (1994) Correlating tool wear, tool life, surface roughness and tool vibration in finish turning with coated carbide tools. Wear 173(1–2):137–144
5. Jang DY, Choi YG, Kim HG, Hsiao A (1996) Study of the correlation between surface roughness and cutting vibrations to develop an on-line roughness measuring technique in hard turning. Int J Mach Tools Manuf 36:453–464
6. Kirby ED, Chen JC, Zhang JZ (2006) Development of a fuzzy-nets-based in-process surface roughness adaptive control system in turning operations. Expert Syst Appl 30(4):592–604
7. Ghani AK, Choudhury IA (2002) Study of tool life, surface roughness and vibration in machining nodular cast iron with ceramic tool. J Mater Process Technol 127:17–22
8. Abouelatta OB, Mádl J (2001) Surface roughness prediction based on cutting parameters and tool vibrations in turning operations. J Mater Process Technol 118(1–3):269–277
9. Huang LH, Chen JC (2001) A multiple regression model to predict in-process surface roughness in turning operation via accelerometer. J Ind Technol 17(2):1–8
10. Beauchamp Y, Thomas M, Youssef AY, Masounave J (1995) Investigation of cutting parameter effects on surface roughness in lathe boring operation by use of a full factorial design. Comput Ind Eng 31(3–4):645–651

11. Thomas M, Beauchamp Y, Youssef AY, Masounave J (1996) Effect of tool vibrations on surface roughness during lathe dry turning process. Comput Ind Eng 31(3–4): 637–644
12. Cheung CF, Lee WB (2000) A multi-spectrum analysis of surface roughness formation in ultra-precision machining. Precis Eng 24(1):77–87
13. Thomas M, Beauchamp Y (2003) Statistical investigation of modal parameters of cutting tools in dry turning. Int J Mach Tools Manuf 43(11):1093–1106
14. Risbood KA, Dixit US, Sahasrabudhe AD (2003) Prediction of surface roughness and dimensional deviation by measuring cutting forces and vibrations in turning. J Mater Process Technol 132(1–3):203–214
15. Podsiadlo P, Stachowiak GW (2005) Development of advanced quantitative analysis methods for wear particle characterization and classification to aid tribological system diagnosis. Tribol Int 38:887–897
16. Kirby ED, Chen JC (2007) Development of a fuzzy-nets-based surface roughness prediction system in turning operations. Comput Ind Eng 53:30–42
17. Bernardos PG, Vosniakos GC (2003) Predicting surface roughness in machining: a review. Int J Mach Tools Manuf 43:833–844
18. Jang DY, Seireg A (1989) Dynamic simulation for predicting surface roughness in turning. ASME Mach Dyn Appl Vib Control Probl 18(2):31–36
19. Kirby ED, Zhang Z, Chen JC (2004) Development of an accelerometer-based surface roughness prediction system in turning operations using multiple regression techniques. J Ind Technol 20(4):1–8
20. Thomas M, Beauchamp Y, Youssef YA (1996) Effect of lathe boring cutting parameters on surface roughness and tool dynamic forces. In: Proceedings of the 13th symposium on engineering applications of mechanics, manufacturing science and engineering. Canadian Society of Mechanical Engineering, Kingston, pp 521–527
21. Hertzsch A, Kröger K, Truckenbrodt H (2002) Microtopographic analysis of turned surfaces by model-based scatterometry. Precis Eng 26(3):306–313
22. Salgado DR, Alonso FJ (2006) Tool wear detection in turning operations using singular spectrum analysis, J Mater Process Technol 171(3):451–458
23. Golyandina N, Nekrutkin V, Zhigljavsky A (2001) Analysss of time series structure—SSA and related techniques. Chapman & Hall/CRC, Boca Raton
24. Wang WJ, Chen J, Wu XK (2001) The application of some non-linear methods in rotating machinery fault diagnosis. Mech Syst Signal Process 15:697–705
25. Alonso FJ, Salgado DR (2005) Application of singular spectrum analysis to tool wear detection using sound signals. Proc IMechE J Eng Manuf 219(9):703–710
26. Salgado DR, Alonso FJ (2007) An approach based on current and sound signals for in-process tool wear monitoring. Int J Mach Tools Manuf. doi:10.1016/j.ijmachtools.2007.04.013
27. Dimla DE (2002) The correlation of vibration signal features to cutting tool wear in a metal turning operation. Int J Adv Manuf Technol 19:705–713
28. Suykens JAK, Vandewalle J (1999) Least squares support vector machine classifiers. Neural Process Lett 9(3):293–300
29. Van Gestel T, Suykens J, Baesens B, Viaene S, Vanthienen J, Dedene G, De Moor B, Vandewalle J (2004) Benchmarking least squares support vector machine classifiers. Mach Learn 54(1):5–32
30. Evgeniou T, Pontil M, Poggio T (2000) Regularization networks and support vector machines. Adv Comput Math 13(1):1–50
31. Mika S, Rätsch G, Weston J, Schölkopf B, Müller KR (1999) Fisher discriminant analysis with kernels. In: IEEE international workshop on neural networks for signal processing. IEEE, Piscataway, pp 41–48
32. Vapnik VN (1999) The nature of statistical learning theory. Springer, New York
33. Shi D, Gindy NN (2007) Tool wear predictive model based on least squares support vector machines. Mech Syst Signal Process 21(4):1799–1814
34. Sun J, Hong GS, Wong YS, Rahman M, Wang ZG (2006) Effective training data selection in tool condition monitoring system. Int J Mach Tools Manuf 46(2):218–224
35. Sun J, Rahman M, Wong YS, Hong GS (2004) Multiclassification of tool wear with support vector machine by manufacturing loss consideration. Int J Mach Tools Manuf 44(11): 1179–1187
36. Luo GY, Osypiw D, Irle M (2003) Surface quality monitoring for process control by on-line vibration analysis using an adaptive spline wavelet algorithm. J Sound Vib 263(1):85–111